NASA Technical Memorandum 102510
ICOMP-90-05

Conditions at the Downstream Boundary for Simulations of Viscous Incompressible Flow

Thomas Hagstrom
State University of New York at Stony Brook
Stony Brook, New York

and Institute for Computational Mechanics in Propulsion
Lewis Research Center
Cleveland, Ohio

February 1990

NASA

Conditions at the Downstream Boundary for Simulations of Viscous, Incompressible Flow

Thomas Hagstrom*
Department of Applied Mathematics and Statistics
State University of New York at Stony Brook
Stony Brook, New York 11794

and Institute for Computational Mechanics in Propulsion
Lewis Research Center
Cleveland, Ohio 44135

Abstract

The proper specification of boundary conditions at artificial boundaries for the simulation of time-dependent fluid flows has long been a matter of controversy. In this work we apply the general theory of asymptotic boundary conditions for dissipative waves, developed by the author in [8], to the design of simple, accurate conditions at a downstream boundary for incompressible flows. For Reynolds numbers far enough below the critical value for linear stability, a scaling is introduced which greatly simplifies the construction of the asymptotic conditions. Numerical experiments with the nonlinear dynamics of vortical disturbances to plane Poiseuille flow are presented which illustrate the accuracy of our approach. The consequences of directly applying the scalings to the equations are also considered.

1 Introduction

Problems posed on unbounded domains are ubiquitous in theoretical and applied fluid mechanics. Examples include exterior domains, as arise in aerodynamics, and cylindrical domains, as are found in the study of internal flows. Numerical simulations require a finite computational mesh which is typically obtained by introducing an artificial boundary. The proper specification of boundary conditions there has long been a matter of

*Supported, in part, by Space Act Agreement C-99066-G and by NSF Grant No. DMS-8905314.

controversy. Their choice is often made on the basis of ad hoc reasoning and their effect on the solution not fully determined.

In [8] the author develops a general theory of asymptotic boundary conditions for linear, dissipative wave propagation problems. The basic approach is to numerically identify dominant wave groups and construct linear approximations to the dispersion relation which are valid in the neighborhood of the dominant waves. These lead to simple, local boundary operators. Error estimates for the truncated problem are derived which establish convergence as the size of the computational domain is increased. The goal of this work is to apply the general theory to the linearized, incompressible Navier-Stokes equations and to test it in fully nonlinear simulations.

In Section 2 we outline the construction of the asymptotic expansions and boundary conditions for the linearized Navier-Stokes equations. Simplified approximations to the full theory, valid for moderate to large Reynolds numbers, are also constructed. These lead to boundary conditions involving fixed constants and a parametric dependence on Reynolds number. The simplifications are based on a simple scaling argument. In Section 3 we carry out the numerical computation of the asymptotic boundary operators for the special case of linearizations about plane Poiseuille flow. Both the simplified and full theory are considered, the latter to validate the approximations leading to the former. Numerical experiments with the nonlinear dynamics of vortical disturbances are presented. These verify the accuracy of our approach even for large amplitude perturbations. Comparisons with the solution on an extended domain are given to study the decay of the error with increasing domain size. Finally, in Section 4, we develop an alternate approach based on the direct introduction of the scalings used to simplify the asymptotic analysis. This leads to a simple set of boundary conditions previously considered by Naughton [13].

Boundary conditions for similar equations based on the analysis of linearizations about homogeneous base flows have been derived by Halpern [9] and Halpern and Schatzman [10]. Related techniques have been employed by Abarbanel and coworkers [1] for the compressible Navier-Stokes equations, by Fasel [7] for simulations of transition and by Ache [2] for steady flows. More recently, Danabasoglu and coworkers [5] have investigated the effect of outflow conditions on the simulation of spatially evolving instabilities.

2 Construction of asymptotic boundary conditions for the incompressible Navier-Stokes equations

2.1 Asymptotic analysis

We consider the incompressible Navier-Stokes equations linearized about plane parallel flow:

$$\begin{aligned} \frac{\partial \omega}{\partial t} + U(y)\frac{\partial \omega}{\partial x} - U''(y)\frac{\partial \psi}{\partial x} &= \frac{1}{Re_l}\left(\frac{\partial^2 \omega}{\partial x^2} + \frac{\partial^2 \omega}{\partial y^2}\right) \\ &\quad + \frac{1}{Re_t}\frac{\partial^2}{\partial y^2}\left(D(y)\omega\right) - \frac{1}{Re_t}D''(y)\frac{\partial^2 \psi}{\partial x^2}, \end{aligned} \tag{1}$$

$$\omega = \frac{\partial^2 \psi}{\partial x^2} + \frac{\partial^2 \psi}{\partial y^2}, \tag{2}$$

$$(x, y) \in (0, \infty) \times (y_0, y_1), \tag{3}$$

$$\psi = \frac{\partial \psi}{\partial y} = 0, \quad y = y_0, y_1. \tag{4}$$

$$\psi(0, y, t) = g_0(y, t), \quad \omega(0, y, t) = g_1(y, t). \tag{5}$$

Here, ψ is the stream function perturbation, ω is the vorticity perturbation and $U(y)$ is the parallel base flow. For generality we have included eddy viscosity terms consistent with a simple mixing length model. (See, e.g., Stanisic [14].) Re_l is, then, a Reynolds number based on the mean flow and the kinematic viscosity while Re_t is a turbulence Reynolds number. An unbounded domain in y could also be considered.

Equations (1-5) are meant to model the 'far field' for a more complicated and general class of problems. Our goal is to derive reasonably simple but accurate boundary conditions at a downstream boundary, $x = \tau$. The general approach to the construction of asymptotic boundary conditions given in [8] may be directly applied in this case. To begin we consider the eigenvalue problem:

$$\begin{aligned} s\hat{\omega} + \lambda U(y)\hat{\omega} - \lambda U''(y)\hat{\psi} &= \frac{1}{Re_l}\left(\lambda^2 \hat{\omega} + \frac{\partial^2 \hat{\omega}}{\partial y^2}\right) \\ &\quad + \frac{1}{Re_t}\frac{\partial^2}{\partial y^2}\left(D(y)\hat{\omega}\right) - \frac{\lambda^2}{Re_t}D''(y)\hat{\psi}, \end{aligned} \tag{6}$$

$$\hat{\omega} = \lambda^2 \hat{\psi} + \frac{\partial^2 \hat{\psi}}{\partial y^2}. \tag{7}$$

The equations above are well known in the theory of hydrodynamic stability and are usually referred to as the spatial Orr-Sommerfeld equations. Techniques for their numerical and asymptotic analysis have been extensively developed. (See, e.g. Drazin and Reid [6]).

Solutions to the linearized problem may be expressed in terms of pairs,

$$\left(\lambda_l(s), \begin{pmatrix} \hat{\omega}_l(y;s) \\ \hat{\psi}_l(y;s) \end{pmatrix}\right), \tag{8}$$

satisfying $\Re(\lambda_l(s)) < 0$ for $\Re(s)$ sufficiently large. We have:

$$\begin{pmatrix} \omega \\ \psi \end{pmatrix} = \sum_l \Phi_l, \tag{9}$$

$$\Phi_l = \int_0^t c_l(p) q_l(x, y, t-p) dp, \tag{10}$$

$$q_l(x, y, t) = \frac{1}{2\pi i} \int_C e^{st + \lambda_l(s)x} \begin{pmatrix} \hat{\omega}_l(y;s) \\ \hat{\psi}_l(y;s) \end{pmatrix} ds. \tag{11}$$

Here C is an appropriate inversion contour.

By a standard steepest descent computation we formally obtain:

$$q_l(x, y, t) \sim \frac{e^{x(s^*(\gamma)\gamma + \lambda_l(s^*(\gamma)))}}{\sqrt{2\pi \lambda_l''(s^*(\gamma))x}} \begin{pmatrix} \hat{\omega}_l(y; s^*(\gamma)) \\ \hat{\psi}_l(y; s^*(\gamma)) \end{pmatrix}, \tag{12}$$

where

$$\gamma = \frac{t}{x}, \quad x \gg 1, \tag{13}$$

and s^* satisfies:

$$\lambda_l'(s^*) = -\gamma, \quad \Re(\gamma) \geq 0, \quad \Im(\gamma) = 0. \tag{14}$$

Substituting the asymptotic expansion of q_l into (10) yields an approximation to Φ_l. The expansion itself may be interpreted as a description of wave packets moving at their group velocity, $\frac{1}{\gamma}$. The formula for Φ_l is then a superposition of wave groups generated at various times.

In contrast with the usual problems in dispersive wave propagation, our generalized wave groups decay (or grow) exponentially as they propagate with a rate:

$$\mu_l(\gamma) = \Re(s^*(\gamma)\gamma + \lambda_l(s^*(\gamma))) \neq 0. \tag{15}$$

We exploit this property to restrict our attention to a small number of dominant wave groups. That is, we expect the signal far downstream to be dominated by wave groups for which μ_l is maximized. Differentiating with respect to γ and using (14) we find a necessary condition for a local maximum:

$$\mu_l'(\gamma) = \Re(s^*(\gamma)) = 0. \tag{16}$$

Let $\tilde{\gamma}_l$ correspond to a global maximum of μ_l. The exact, nonlocal boundary condition satisfied by q_l is given in transform space by:

$$\left(\frac{\partial}{\partial x} - \lambda_l(s)\right) \hat{q}_l = 0. \tag{17}$$

We approximate it by replacing λ_l by the linear part of its Taylor series at $s^*(\tilde{\gamma}_l)$. This leads to a local condition:

$$\left(\frac{\partial}{\partial x} - \lambda_l(s^*(\tilde{\gamma}_l)) - \lambda_l'(s^*(\tilde{\gamma}_l))(\frac{\partial}{\partial t} - s^*(\tilde{\gamma}_l))\right) \Phi_l = 0. \tag{18}$$

This operator may be directly applied to $\begin{pmatrix} \omega \\ \psi \end{pmatrix}$ if it corresponds to a maximum over all l. More generally, an operator may be constructed as the product of operators taken from a few modes and local maxima.

We summarize below a procedure for constructing the asymptotic boundary conditions:

- Compute local minima of the decay rates, $-\mu_l$. That is compute solutions of (14) and (16).
- Choose from these a small subset, $(\tilde{s}_j, l_j)$, including the overall minimum decay rate as well as any other wave groups whose decay rate is close enough to the minimum.
- Use as the boundary condition at $x = \tau$:

$$\prod_j \left(\frac{\partial}{\partial x} - \lambda_{l_j}(\tilde{s}_j) - \lambda_{l_j}'(\tilde{s}_j)(\frac{\partial}{\partial t} - \tilde{s}_j)\right) \begin{pmatrix} \omega \\ \psi \end{pmatrix} \equiv B \begin{pmatrix} \omega \\ \psi \end{pmatrix} = \begin{pmatrix} 0 \\ 0 \end{pmatrix}. \tag{19}$$

In [8] an error analysis is developed for this procedure. The main result is that the difference, e, between the solution on the truncated domain and the true unbounded domain solution satisfies:

$$\|e\| = O(\frac{e^{\mu_0 \tau}}{\tau}), \quad \tau \to \infty. \tag{20}$$

Here,

$$\mu_0 = \max_{l,\gamma} \mu_l(\gamma). \tag{21}$$

Although this result was obtained under fairly general hypotheses, we have been unable to verify them in this case. The error estimate is, however, consistent with the computational experiments we will present.

In order to directly complete the search for the dominant wave groups, the repeated numerical solution of (6-7) in conjunction with a line search procedure is required. We have implemented an algorithm to accomplish this using a spectral discretization of the Orr-Sommerfeld problem [4]. This will be discussed in greater detail in the context of the numerical experiments.

2.2 Simplified approximations

Despite the availability of a number of appropriate techniques, the direct numerical approach to the construction of the asymptotic boundary conditions has certain drawbacks. Among these are the expense of the computation and the need to recompute the boundary condition as the Reynolds number(s) change. Consequently, we have developed an alternate procedure based on the asymptotic analysis of (6-7) for $Re_{t,l}$ large. The assumption underlying this analysis is:

Assumption 1 *The dominant wave groups satisfy:*

$$\tilde{s} = 0. \tag{22}$$

We note that this condition does *not* necessarily hold for all Reynolds numbers. In particular, near the critical Reynolds number from linear stability theory the dominant wave group corresponds to the critical Tollmien-Schlichting waves which, in general, do not have $s^* = 0$. For the special case of Poiseuille flow, which we have used for numerical experimentation, we find that Assumption 1 holds for a wide range of subcritical values of Re_l.

By itself Assumption 1 allows the construction of the asymptotic boundary conditions using a single solution of the Orr-Sommerfeld equations. Furthermore, the *necessary* condition for its validity, (14), can be directly verified. Further simplification occurs when we consider an expansion of the solution of (6-7) in powers of $\frac{1}{Re_t}$. (For laminar flows this is replaced by an expansion in $\frac{1}{Re_l}$). We take:

$$\lambda = \frac{\bar{\lambda}}{Re_t}, \quad s = \frac{\bar{s}}{Re_t}. \tag{23}$$

To leading order the eigenvalue problem becomes:

$$\bar{\lambda}\left(U(y)\frac{\partial^2}{\partial y^2} - U''(y)\right)\hat{\psi} = \left(\frac{\partial^2}{\partial y^2}(D(y) + \epsilon_l)\frac{\partial^2}{\partial y^2} - \bar{s}\frac{\partial^2}{\partial y^2}\right)\hat{\psi}, \tag{24}$$

where we have made the substitution

$$\hat{\omega} = \frac{\partial^2 \hat{\psi}}{\partial y^2}, \tag{25}$$

and

$$\epsilon_l = \frac{Re_t}{Re_l}. \tag{26}$$

We may now proceed to construct the asymptotic boundary conditons based on a numerical analysis of (24) with Assumption 1. We emphasize the advantages of this simplification:

- We need only solve (24) once for $\bar{s} = 0$ and then compute the required derivatives, $\frac{d\bar{\lambda}}{d\bar{s}}$.
- The resulting boundary conditions depend algebraically on the Reynolds number.

Unfortunately, (24) with $\bar{s} = 0$ is not self-adjoint, so it is difficult to obtain general results on its solutions. An ideal result would guarantee the existence of solutions with real, positive group velocity. We note that a real group velocity is guaranteed for real eigenvalues. It is tempting to rewrite the troublesome term, $U\frac{\partial^2}{\partial y^2}$, as its symmetric part plus a perturbation, but the unbounded 'perturbation' is too large for the direct application of the general theory (Kato [12]). It is possible to derive some simple equations for the real and imaginary parts of $\bar{\lambda}$:

$$\Re(\bar{\lambda}) = \frac{-I_0}{\left(I_1 + I_2 + \frac{I_3^2}{I_1}\right)}, \tag{27}$$

$$\Im(\bar{\lambda}) = -\Re(\bar{\lambda})\frac{I_3}{I_1}, \tag{28}$$

where

$$I_0 = \int_{y_0}^{y_1} (D(y) + \epsilon_l)|\psi''|^2 dy, \tag{29}$$

$$I_1 = \int_{y_0}^{y_1} U(y)|\psi'|^2 dy, \tag{30}$$

$$I_2 = \frac{1}{2}\int_{y_0}^{y_1} U''(y)|\psi|^2 dy, \tag{31}$$

$$I_3 = \Im(\int_{y_0}^{y_1} U'(y)\psi^*\psi' dy). \tag{32}$$

These relations suggest that all but finitely many eigenvalues will have negative real part and that they cannot lie too far from the real axis. For the special case of Poiseuille flow; $y_0 = -1$, $y_1 = 1$ and $U = 1 - y^2$, our numerical solution of (24) indicates that *all* eigenvalues are real and negative and that the group velocities are positive. Again, these conditions may be checked in the general case by a single solution of (24). The computational cost of this procedure is then negligible in comparison with that of the full simulations.

3 Numerical experiments: the dynamics of some vortical disturbances to plane Poiseuille flow

In this section we describe the results of numerical experiments with the asymptotic boundary conditions we have developed. We take our base flow to be laminar channel

flow:

$$U(y) = 1 - y^2, \quad y \in (-1, 1), \tag{33}$$

and consider (1) without the eddy viscosity terms. (That is, $D = 0$ and $Re = Re_l$.) We divide our discussion into two parts considering first the eigenvalue problems used to construct the asymptotic boundary conditions and, then, the use of these conditions in the simulation of the full nonlinear equations.

3.1 Numerical analysis of the full and reduced eigenvalue problems

We have developed two separate programs for the computation of the various quantities defining the boundary conditions. The first solves a discrete approximation to the reduced eigenvalue problem (24) with $\bar{s} = 0$ to find λ and $\frac{d\lambda}{ds}$. It is the simplified condition defined by this reduced problem which is used in the simulations. The second solves a discrete (pseudospectral) approximation to the full spatial Orr-Sommerfeld equations, (6-7), and also computes the group velocities. The results of the latter are used to validate the use of the reduced equations for moderate Reynolds numbers. In practice, the point of the approximations leading to (24) is to avoid the expense of solving (6-7), and we show that this is justified in the case of Poiseuille flow for Re large enough compared to 1 but far enough below $Re_{crit} \approx 5775$. For larger values of Re the full eigenvalue problem must be used.

Approximating (24) we introduce a uniform mesh, $y_i = -1 + ih$, $i = 1, \ldots, N$, $h = \frac{2}{N+1}$. Denote by $\hat{\Psi}_i$ the approximation to $\hat{\psi}(y_i)$. Using second order centered difference approximations to the derivatives we have:

$$\bar{\lambda}\left(2\hat{\Psi}_i + (1 - y_i^2)D_+D_-\hat{\Psi}_i\right) = (D_+D_-)^2\hat{\Psi}_i, \tag{34}$$

where

$$D_+D_-\hat{\Psi}_i = \frac{(\hat{\Psi}_{i+1} - 2\hat{\Psi}_i + \hat{\Psi}_{i-1})}{h^2}, \tag{35}$$

$$(D_+D_-)^2\hat{\Psi}_i = \frac{(\hat{\Psi}_{i+2} - 4\hat{\Psi}_{i+1} + 6\hat{\Psi}_i - 4\hat{\Psi}_{i-1} + \hat{\Psi}_{i-2})}{h^4}. \tag{36}$$

These are supplemented by the discrete wall conditions:

$$\hat{\Psi}_0 = \hat{\Psi}_{N+1} = 0, \tag{37}$$

$$\hat{\Psi}_{-1} = \hat{\Psi}_1, \quad \hat{\Psi}_{N+2} = \hat{\Psi}_N. \tag{38}$$

λ	$\frac{d\lambda}{ds}$
-21.659	-1.999
-28.111	-1.384
-72.694	-1.991
-85.178	-1.430

Table 1: Dominant eigenvalues

The eigenvalues and eigenvectors of the resulting generalized matrix eigenvalue problem were computed using the IMSL subroutine EIGZF. To compute $\frac{d\bar{\lambda}}{d\bar{s}} = \frac{d\lambda}{ds}$ we differentiate (24) with respect to $\bar{s}$ to obtain:

$$\left(\bar{\lambda}_l L - M\right) \frac{d\hat{\psi}_l}{d\bar{s}} = -\frac{d\bar{\lambda}_l}{d\bar{s}} L\hat{\psi}_l - \frac{\partial^2 \hat{\psi}_l}{\partial y^2}. \tag{39}$$

Here L and M are, respectively, the partial differential operators appearing on the left and right hand sides of (24) with $\bar{s} = 0$. Multiplying this equation by an adjoint eigenfunction and integrating leads to an expression for $\frac{d\bar{\lambda}}{d\bar{s}}$. For the discrete approximation we simply use the original difference approximation to L and D_+D_- for $\frac{\partial^2}{\partial y^2}$. Left eigenvectors, $\hat{\Upsilon}$, were computed by inverting the matrix of right eigenvectors and were then used to compute $\frac{d\lambda}{ds}$:

$$\frac{d\lambda}{ds} = -\frac{\sum_i \hat{\Upsilon}_i D_+ D_- \hat{\Psi}_i}{\sum_i \hat{\Upsilon}_i \left(2\hat{\Psi}_i + (1-y_i^2) D_+ D_- \hat{\Psi}_i\right)}. \tag{40}$$

All eigenvalues were found to be real and negative. Tabulated are the six smallest eigenvalues along with the corresponding values of $\frac{d\lambda}{ds}$. For these we have $N = 39$. Their accuracy may be verified by comparing with solutions of the full Orr-Sommerfeld equation for $s = 0$ published by Bramley and Dennis [3].

The first and third eigenvalues correspond to even stream function perturbations while the second and fourth correspond to odd perturbations. It is interesting to note that the group velocities, $-(\frac{d\lambda}{ds})^{-1}$, are nearly equal within each symmetry class. In the experiments which follow a product boundary condition based on the first two modes is employed. This is formally justified if $e^{\frac{-28.111\tau}{Re}} \gg e^{\frac{-72.694\tau}{Re}}$ However, the near equality of the group velocities is likely to extend the range for which the two mode condition is reasonably accurate.

It is of some interest to view the flow field which results from adding to Poiseuille flow the asymptotic solution corresponding to the first symmetric and antisymmetric eigenfunctions. These are shown in Figure 1 for $Re = 100$, $c = A\delta(t - t_0)$, $t = t_0 + 3$.

It must be emphasized that the amplitude of the perturbation, A, is here chosen to be much larger than a linearized analysis can reasonably allow. Nonetheless, the streamlines bear interesting similarities to those we have obtained in full nonlinear simulations.

Although the solutions of the reduced eigenvalue problem described above satisfy *necessary*, local conditions for dominant wave groups, *sufficient* conditions are global and more difficult to check. Indeed, it is well known that Poiseuille flow becomes linearly unstable for $Re \approx 5775$ [6]. Then the dominant wave groups are expected to grow in space, while those above decay. In order to further investigate the dominance of the solutions of the reduced problem for subcritical Reynolds numbers, as well as compute the asymptotic boundary conditions for higher Reynolds numbers, approximate solutions of the full spatial Orr-Sommerfeld equation were computed.

The mesh points are taken to be the Chebyshev nodes:

$$y_i = \cos\left(\frac{\pi(i-1)}{N}\right), \quad i = 1, \ldots, N+1. \tag{41}$$

The ijth component of the $(N-1) \times (N-1)$ differentiation matrix D_1 is defined by:

- Let $P_j(y)$ be the polynomial of degree N which is 1 at $y = y_{j+1}$ and 0 at the other nodes.
- Let $(D_1)_{ij} = P_j'(y_{i+1})$, $i, j = 1, \ldots, N-1$.

The ijth component of the $(N+1) \times (N+1)$ differentiation matrix D_2 is defined by:

- Let $P_j(y)$ be the polynomial of degree N which is 1 at $y = y_j$ and 0 at the other nodes.
- Let $(D_2)_{ij} = P_j''(y_i)$, $i, j = 1, \ldots N+1$.

Take u_2 to be an $(N+1)$-vector whose ith component approximates $\omega(y_i)$ and $u_1 = \lambda u_2$. Let u_3 be an $(N-1)$-vector whose ith component approximates $\lambda\hat{\psi}(y_{i+1})$ and u_4 the $(N-1)$-vector whose ith component approximates $\hat{\psi}'(y_{i+1})$. Note we are explicitly imposing the boundary conditions that $\hat{\psi}$ and its normal derivatives be zero at $y = \pm 1$. A discrete approximation to the eigenvalue problem (6-7) is then given by:

$$\begin{pmatrix} Re \cdot V & -D_2 + Re \cdot s \cdot I & Re \cdot T & 0 \\ I & 0 & 0 & 0 \\ 0 & W & 0 & D_1 \\ 0 & 0 & -D_1 & 0 \end{pmatrix} \vec{u} = \lambda \vec{u}. \tag{42}$$

Here the $(N+1) \times (N-1)$ matrix T is given by:

$$T = \begin{pmatrix} \vec{0}^T \\ 2I \\ \vec{0}^T \end{pmatrix}, \tag{43}$$

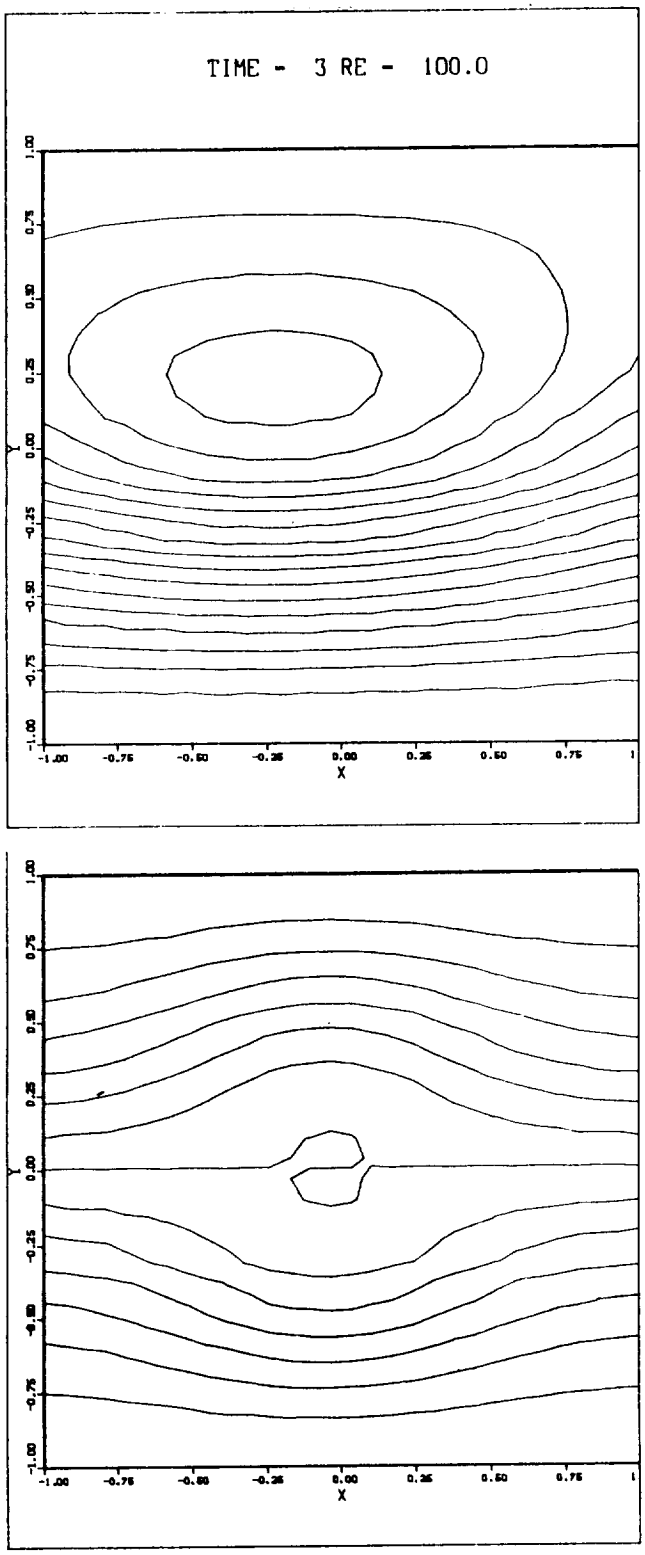

Figure 1: Asymptotic solutions of the linearized problem superposed on Poiseuille flow. The signal data is a $A\delta(\text{TIME})$ and $X = x - \frac{\text{TIME}}{(\frac{d\lambda}{ds})}$.

while the $(N-1) \times (N+1)$ matrix W is given by:

$$W = \begin{pmatrix} \vec{0} & I & \vec{0} \end{pmatrix}. \tag{44}$$

The problem was solved for λ given s using the IMSL subroutine EIGCC. Approximations to $\frac{d\lambda}{ds}$ were also computed following the same ideas used for the simplified eigenproblem.

A (coarse) sampling of Reynolds numbers between 100 and 6000 was taken. For each value of Re solutions for $s = i\frac{k-1}{10}$, $k = 1, \ldots, 21$ were found. This choice is motivated by (16) and the fact that neutral modes in the classical theory satisfy $|\Im(s)| < 1$ [6]. If the imaginary part of the derivative of any eigenvalue appeared to pass through 0 and the real part of λ was of the same order as the solutions of the reduced problem, the s increments were refined in the appropriate neighborhood. Note that a real $\frac{d\lambda}{ds}$ corresponds to a maximum or minimum of $\Re(\lambda)$ as s varies on the imaginary axis. On the basis of these computations we tentatively conclude that the modes approximated by the reduced eigenvalue problem are dominant for a range of Reynolds numbers including at least the interval $100 \leq Re \leq 4000$.

It is somewhat surprising, and perhaps of some interest in the study of subcritical transition phenomena, that the reduced problem still provides the dominant modes at so high a Reynolds number. For example, for $Re = 4000$ we find that the least damped mode with $s^* \neq 0$ has a decay rate more than one and a half times that of the least damped mode with $s^* = 0$. For $Re = 6000$, on the other hand, there is an eigenvalue with positive real part for $\Im(s)$ in an interval including $(.25, .28)$. The dominant wave group is then described by:

$$s^* \approx .27i, \tag{45}$$

$$\lambda \approx 9.11 \times 10^{-4} - 1.027i, \tag{46}$$

$$\frac{d\lambda}{ds} \approx -.380. \tag{47}$$

3.2 Numerical method

In order to test the proposed boundary conditions, we consider the following problem:

$$\frac{\partial \omega}{\partial t} - \frac{\partial \psi}{\partial y}\frac{\partial \omega}{\partial x} + \frac{\partial \psi}{\partial x}\frac{\partial \omega}{\partial y} = \frac{1}{Re}\left(\frac{\partial^2 \omega}{\partial x^2} + \frac{\partial^2 \omega}{\partial y^2}\right), \tag{48}$$

$$\omega = \frac{\partial^2 \psi}{\partial x^2} + \frac{\partial^2 \psi}{\partial y^2}, \tag{49}$$

$$(x, y) \in (0, \tau) \times (-1, 1), \tag{50}$$

with boundary and initial conditions:

$$\psi(x,y,0) = -y + \frac{y^3}{3}, \quad \omega(x,y,0) = 2y, \tag{51}$$

$$\psi(x,-1,t) = \frac{2}{3}, \quad \psi(x,1,t) = -\frac{2}{3}, \quad \frac{\partial \psi}{\partial y}(x,\pm 1,t) = 0, \tag{52}$$

$$\psi(0,y,t) = g_0(y,t), \quad \omega(0,y,t) = g_1(y,t), \tag{53}$$

$$B\psi(\tau,y,t) = B\left(-y + \frac{y^3}{y}\right), \quad B\omega(\tau,y,t) = B(2y). \tag{54}$$

Here the asymptotic boundary operator B is given by:

$$B = \left(\frac{\partial}{\partial x} - \lambda_1 - \alpha_1 \frac{\partial}{\partial t}\right)\left(\frac{\partial}{\partial x} - \lambda_2 - \alpha_2 \frac{\partial}{\partial t}\right), \tag{55}$$

$$\lambda_1 = -\frac{21.6593}{Re}, \quad \alpha_1 = -1.9990265, \tag{56}$$

$$\lambda_2 = -\frac{28.11134}{Re}, \quad \alpha_2 = -1.383905. \tag{57}$$

A uniform mesh,

$$y_i = -1 + ih, \; i = 1,\ldots,N; \quad x_j = jh, \; j = 1,\ldots M, \tag{58}$$

was introduced and the spatial derivatives replaced by the standard second order central differencing formulas; D_+D_- for the second derivatives and D_0 for the first. Time differencing was Crank-Nicholson for the viscous terms and Adams-Bashforth for the transport terms so that for interior nodes we have:

$$\left(1 - \frac{\delta t}{2Re}\tilde{\nabla}^2\right)\omega^{(t+\delta t)} = \left(1 + \frac{\delta t}{2Re}\tilde{\nabla}^2\right)\omega^{(t)} - \frac{\delta t}{2}(3T^{(t)} - T^{(t-\delta t)}), \tag{59}$$

$$\omega^{(t+\delta t)} = \tilde{\nabla}^2 \psi^{(t+\delta t)}. \tag{60}$$

Here $\tilde{\nabla}^2$ is the discrete Laplacian and $T^{(t)}$ is given by:

$$T^{(t)} = -D_{0y}\psi^{(t)} D_{0x}\omega^{(t)} + D_{0x}\psi^{(t)} D_{0y}\omega^{(t)}. \tag{61}$$

For all our simulations we have taken $\frac{\delta t}{\delta y} = .125$. The wall boundary conditions on ψ are also directly discretized and ω at the wall is computed by (60). The asymptotic boundary condition (54) was replaced by a product of discrete boundary operators following Higdon [11]. A typical term,

$$B_l = \left(\frac{\partial}{\partial x} - \lambda - \alpha \frac{\partial}{\partial t}\right), \tag{62}$$

is approximated by:

$$\tilde{B}_l(v^{(t)}_{(x)}) = \begin{array}{l} \frac{1}{2h}(v^+_+ + v^-_+ - v^+_- - v^-_-) - \frac{\lambda}{4}(v^+_+ + v^-_+ + v^+_- + v^-_-) \\ -\frac{\alpha}{2\delta t}(v^+_+ + v^+_- - v^-_+ - v^-_-), \end{array} \tag{63}$$

where

$$v^{\pm}_{\pm} = v^{(t\pm\frac{\delta t}{2})}_{(x\pm\frac{h}{2})}. \tag{64}$$

Then $\prod B_l$ becomes $\prod \tilde{B}_l$. In the present case we have the product of two first order operators. The resulting discrete operator then involves three mesh lines in x and three time levels.

To solve the linear system required by the implicit time stepping we employed what we believe to be a novel direct method based on discrete separation of variables. That is a method similar to fast solvers for elliptic equations. We begin by diagonalizing a rearrangement of the $2N \times 2N$ matrix:

$$B = \begin{pmatrix} \frac{2Re}{\delta t} I - D_{+y}D_{-y} & 0 \\ I & -D_{+y}D_{-y} \end{pmatrix}. \tag{65}$$

Although B is not symmetric, we find its eigenvalues to be real and positive for $\frac{Re}{\delta t}$ sufficiently large, certainly within the range of problems we have considered. Denote its eigenvalues by κ_i with corresponding right eigenvectors $\vec{r}_i$. Writing,

$$\begin{pmatrix} \omega^{(t+\delta t)} \\ \psi^{(t+\delta t)} \end{pmatrix} = \sum_{i=1}^{2N} c_i^{(t+\delta t)}(x)\vec{r}_i. \tag{66}$$

we obtain an uncoupled collection of tridiagonal systems for the c_i's:

$$(\kappa_i - D_{+x}D_{-x})c_i^{(t+\delta t)} = f_i, \tag{67}$$

where the f_i's are computed from the right hand sides of the implicit time stepping formulas. Note that the boundary conditions at 0 and τ are directly applied to c_i. A formal operation count for this method results in an estimate of $8N^2M + o(N^2M)$ operations per time step, which is the the same as for back substitution with a band solver (without pivoting). However, the preprocessing is likely to be cheaper for our method, at least when M is large enough compared with N (long channels).

3.3 Results

We first present results for $Re = 400$. We take $N = 39$ and consider $\tau = 2, 4, 6$. ($M = 40, 80, 120$.) For purposes of comparison, we also compute a solution with $\tau = 15$,

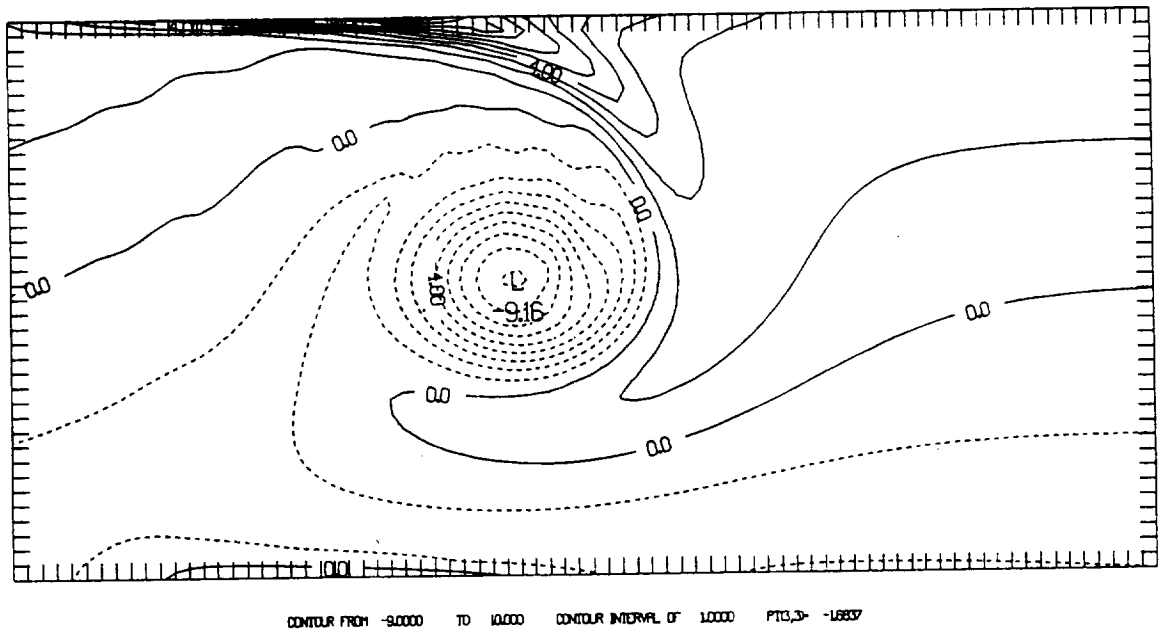

Figure 2: Vorticity contours at $t = 2.5$, $\tau = 15$.

which we will refer to as 'exact', and for $\tau = 4$ with Neumann boundary conditions, $\frac{\partial \psi}{\partial x} = \frac{\partial \omega}{\partial x} = 0$. The inflow perturbations are taken to be:

$$g_0 = -y + \frac{y^3}{3} + \begin{cases} Ae^{-6(y^2+(1-2t)^2)}, & 0 \le t \le 1 \\ 0, & t > 1 \end{cases}, \tag{68}$$

$$g_1 = 2y + \begin{cases} 24Ae^{-6(y^2+(1-2t)^2)}, & 0 \le t \le 1 \\ 0, & t > 1 \end{cases}. \tag{69}$$

Here A is an adjustable amplitude parameter.

Figure 2 depicts vorticity contours at $t = 2.5$ for $\tau = 15$ and $A = \frac{1}{2}$. Note that the flow certainly cannot be considered a small perturbation of Poiseuille flow, so that we cannot expect the linearized analysis leading to the boundary conditions to be valid. We are nonetheless interested in testing the conditions in this nonlinear setting. Figures 3-5 depict the same flow at $t = 6$ as well as simulations with $\tau = 4$ using the asymptotic boundary conditions and Neumann conditions. We see that the exact solution and the one computed with the boundary conditions we propose are virtually indistinguishable, while the flow computed with the Neumann conditions is greatly distorted. Note that the displacement of the vortex causes a large error at the upper wall which extends well back into the computational domain. Figures 6-8 depict the same computations at $t = 7.5$. Although the main disturbance has passed outside the computational domain, the error

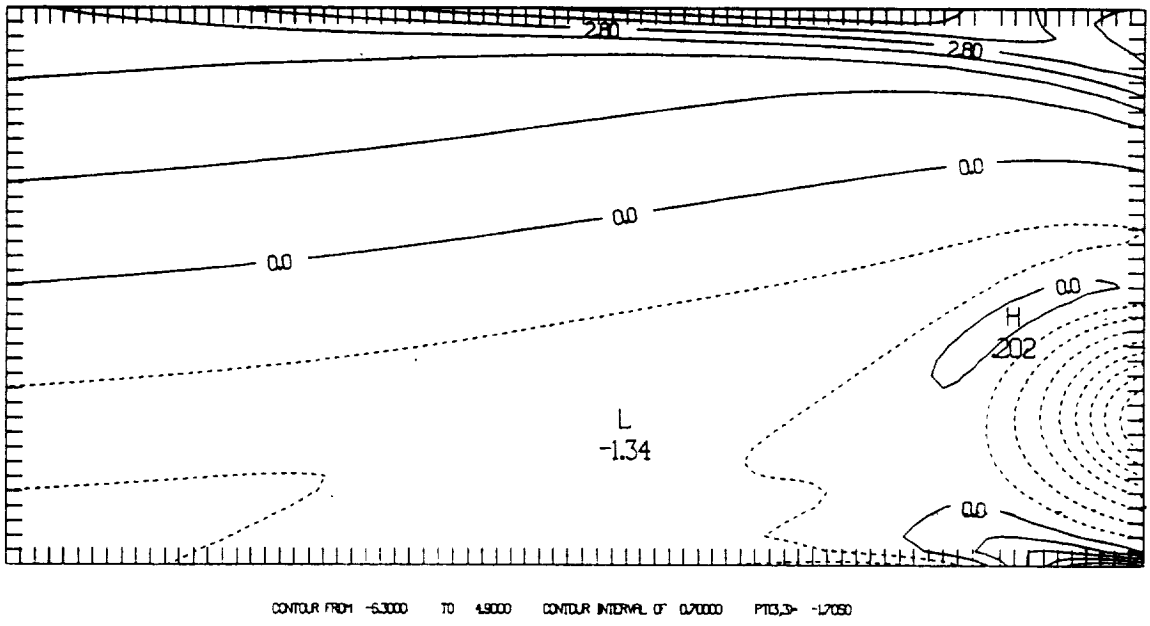

Figure 3: Vorticity contours at $t = 6$, $\tau = 15$.

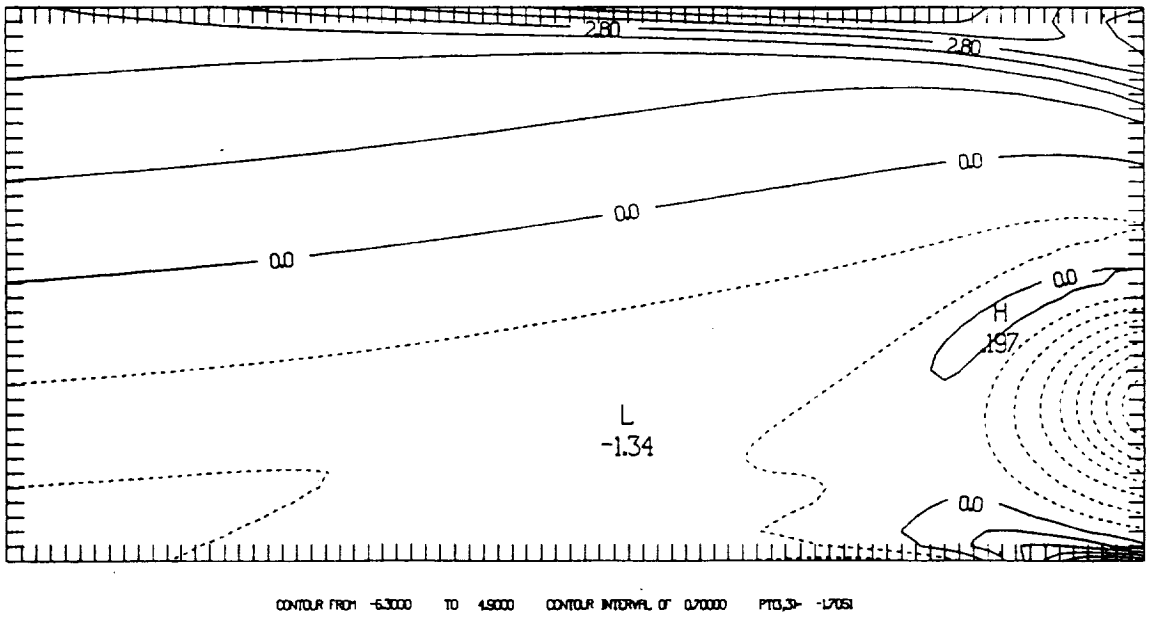

Figure 4: Vorticity contours at $t = 6$, $\tau = 4$, asymptotic conditions.

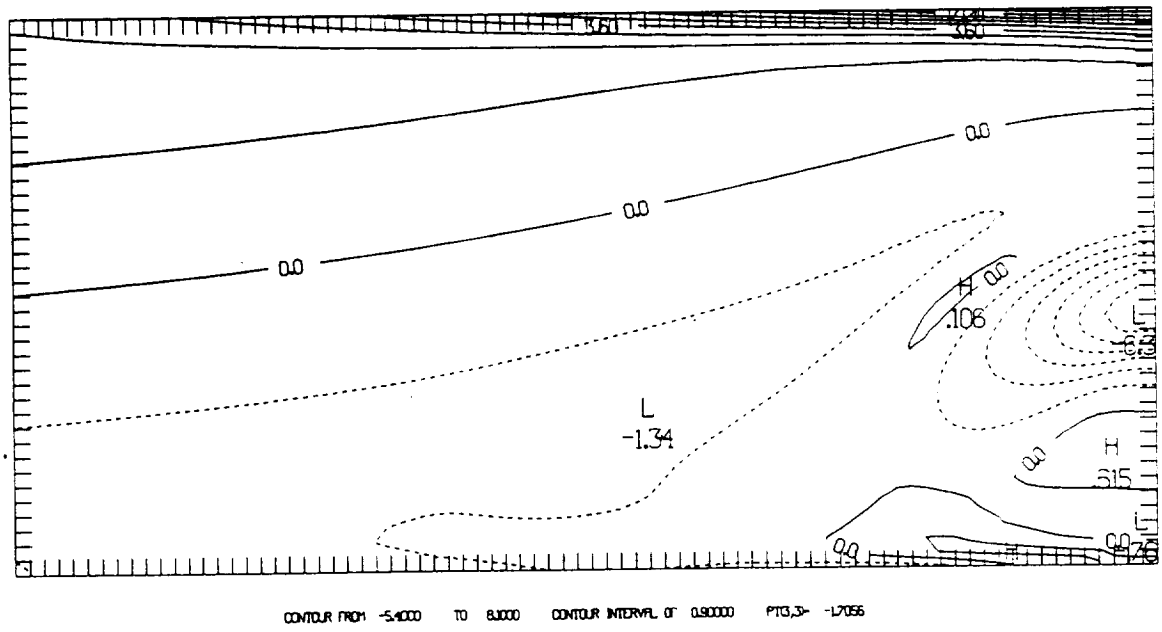

Figure 5: Vorticity contours at $t = 6$, $\tau = 4$, Neumann conditions.

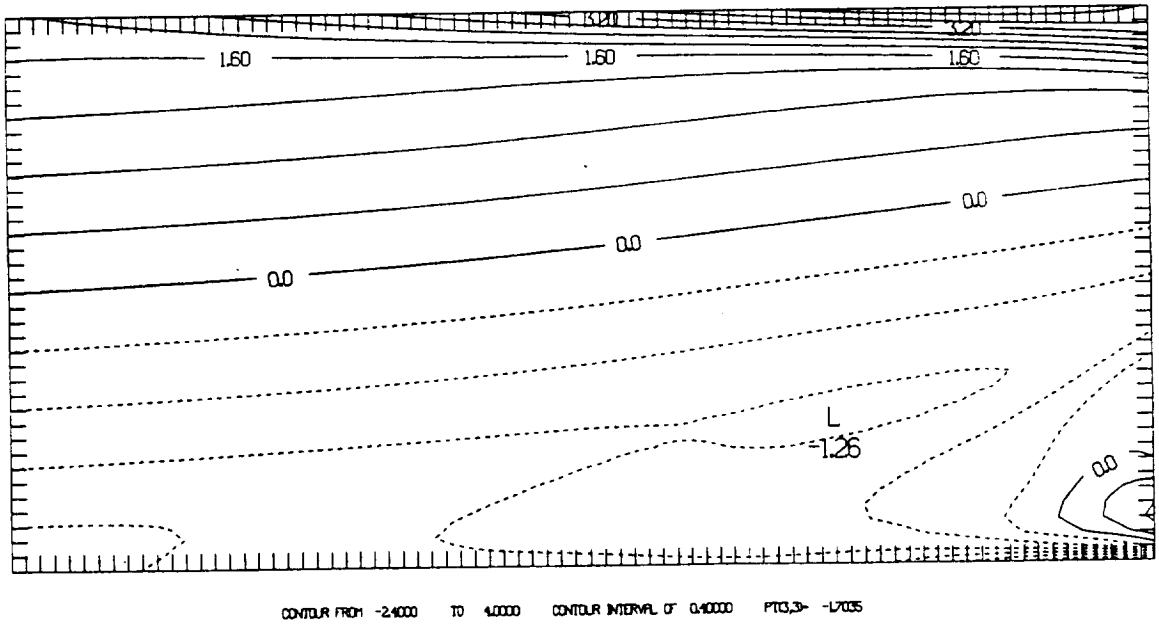

Figure 6: Vorticity contours at $t = 7.5$, $\tau = 15$.

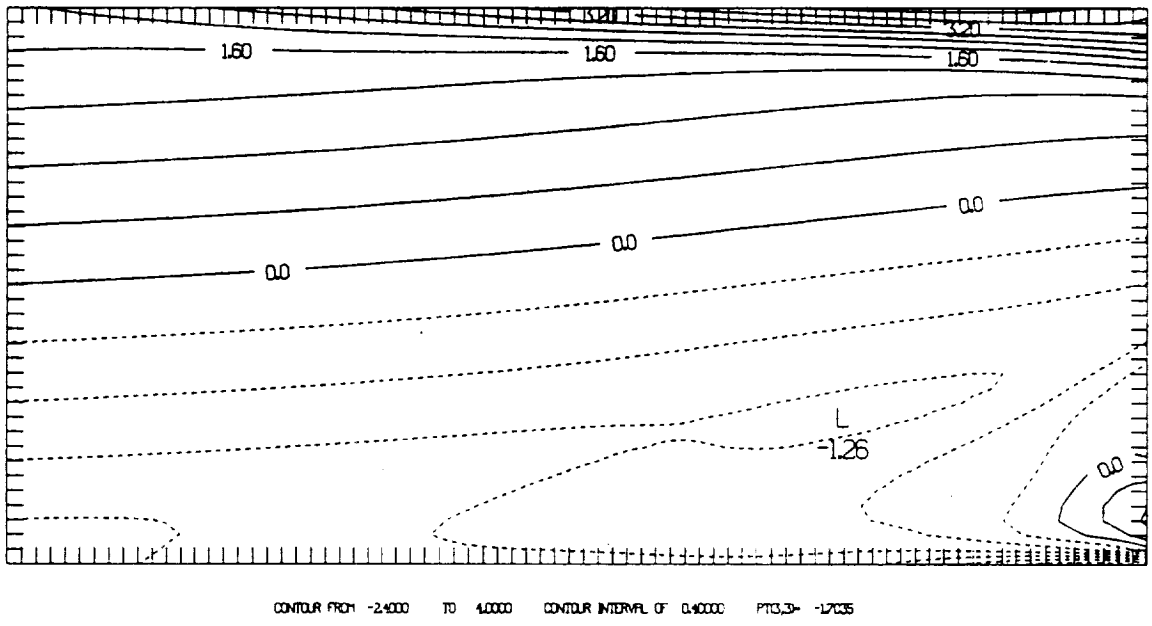

Figure 7: Vorticity contours at $t = 7.5$, $\tau = 4$, asymptotic conditions.

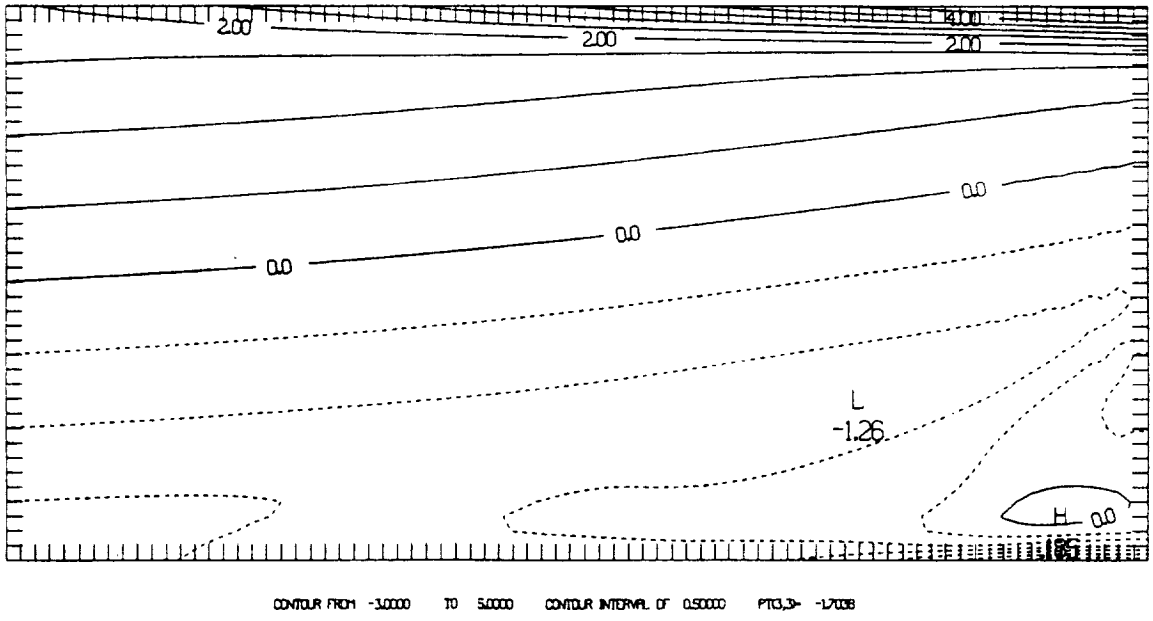

Figure 8: Vorticity contours at $t = 7.5$, $\tau = 4$, Neumann conditions.

A	Boundary Condition	τ	Maximum Error
$\frac{1}{2}$	Asymptotic	2	1.8
$\frac{1}{2}$	Asymptotic	4	.65
$\frac{1}{2}$	Neumann	4	7.0
$\frac{1}{2}$	Asymptotic	6	.42
$\frac{1}{16}$	Asymptotic	2	.12
$\frac{1}{16}$	Asymptotic	4	.018
$\frac{1}{16}$	Asymptotic	6	.013

Table 2: Vorticity errors for $0 \leq t \leq 10$.

at the walls in the Neumann computation is still quite evident.

It is also interesting to look at the maximum errors as a function of τ. Here, again, we take the error to be the difference between the given solution on the truncated domain and the solution for $\tau = 15$. The tabulated results clearly show the decay of the error with increasing τ. Indeed the theory predicts a decrease in error of approximately $\frac{2}{3}$ as τ increases from 4 to 6, and the results show this precisely. This conclusion can only be tentative, however, as at the end of the simulation the disturbance had not fully passed through the boundary in the case of $\tau = 6$. The error decreases much more rapidly as τ increases from 2 to 4, but this is not surprising as our entire construction is dependent on large τ asymptotics.

Nonlinear effects are demonstrated by comparing results for $A = \frac{1}{2}$ with those for $A = \frac{1}{16}$. Although the amplitude is scaled by a factor of 8, the errors scale by factors of 15 to 30. Nonetheless, we are quite surprised by the success of our method in the nonlinear regime. It cannot be explained by our linear analysis. It seems a nonlinear analysis of disturbance propagation is required. This is an interesting topic for future research.

A limited number of simulations have also been carried out at $Re = 2000$ for the same inflow disturbances. Figures 9-10 show vorticity contours at $t = 5.75$ for simulations using, respectively, the asymptotic and Neumann conditions at $\tau = 4$. In this case we have $N = 79$ and $M = 160$. Due to the expense involved, we were unable to carry out a similar simulation on a large domain. Nonetheless, the differences in the vortex dynamics for the two downstream conditions is clear and, apparently, analagous with the results at lower Reynolds number.

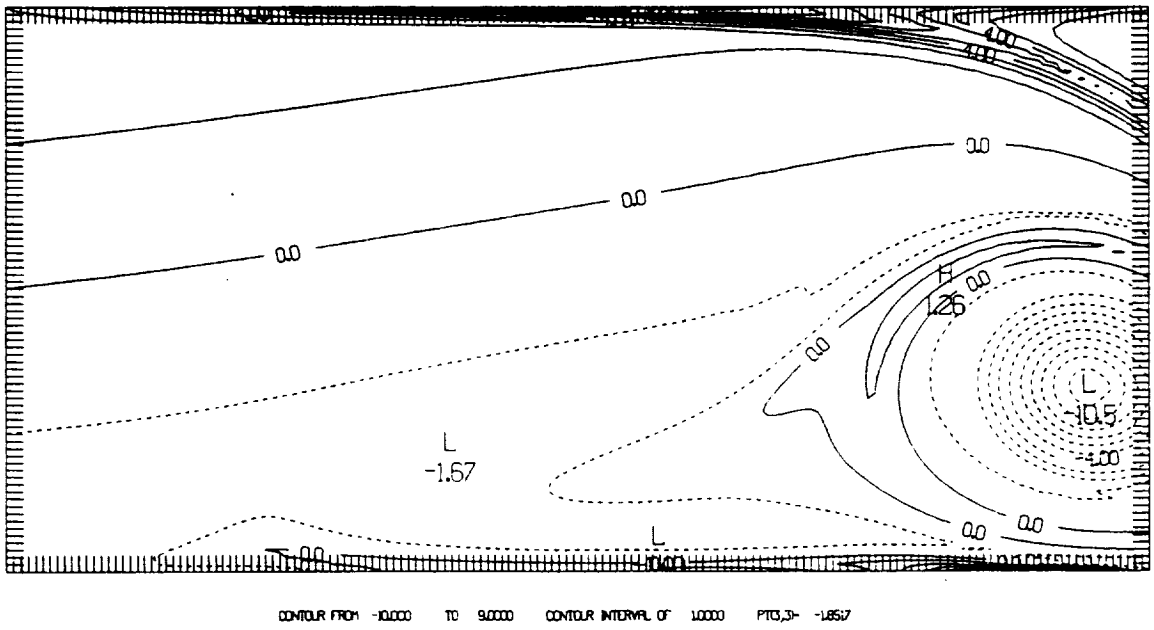

Figure 9: Vorticity contours at $t = 5.75$, $\tau = 4$, asymptotic conditions.

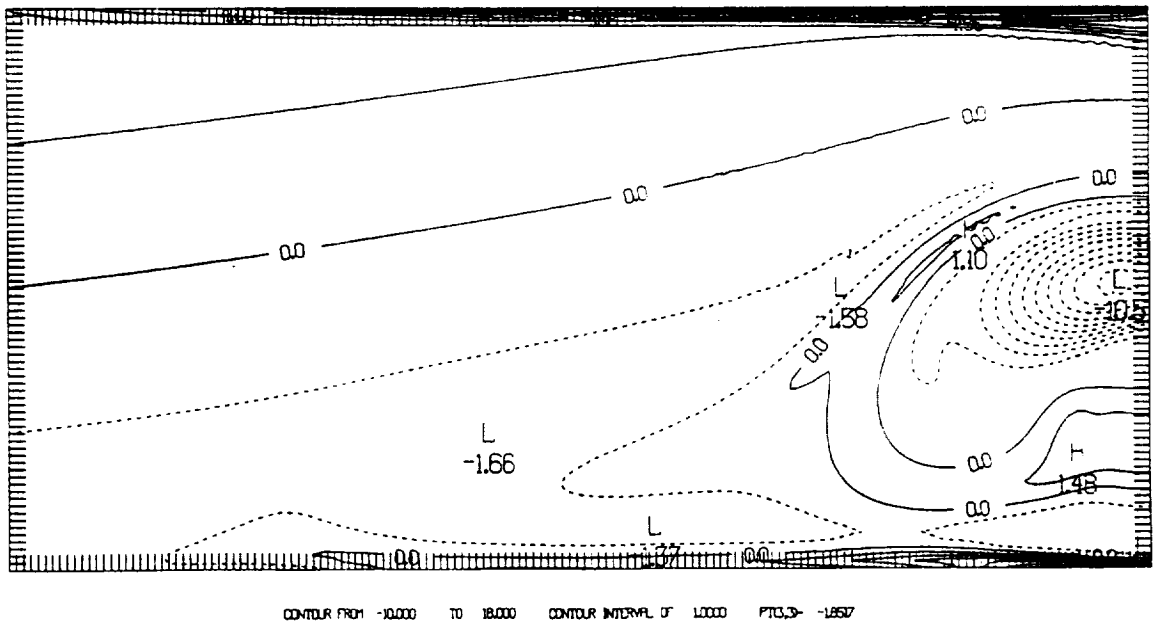

Figure 10: Vorticity contours at $t = 5.75$, $\tau = 4$, Neumann conditions.

4 Primitive Variable Formulation and Direct Application of the Scalings

In this section we discuss the application of the ideas in this paper to the derivation of asymptotic boundary conditions for the primitive variable formulation of the Navier-Stokes equations. We are guided by the theory of boundary conditions for primitive variable formulations which is developed in the doctoral dissertation of Naughton [13]. This theory is based on the construction of energy estimates for the linearized equations. We emphasize that the conditions we will describe have not yet been fully analyzed or implemented.

Linearizing about a parallel flow and assuming, for turbulent flows, a simple eddy viscosity we have:

$$\frac{\partial u}{\partial x} + \frac{\partial v}{\partial y} = 0, \tag{70}$$

$$\begin{aligned} \tfrac{\partial u}{\partial t} + U(y)\tfrac{\partial u}{\partial x} + U'(y)v &= -\tfrac{\partial p}{\partial y} + \tfrac{1}{Re_l}\left(\tfrac{\partial^2 u}{\partial x^2} + \tfrac{\partial^2 u}{\partial y^2}\right) \\ &\quad + \tfrac{1}{Re_t}\left(D(y)\tfrac{\partial^2 u}{\partial x^2} + \tfrac{\partial}{\partial y}(D(y)\tfrac{\partial u}{\partial y})\right), \end{aligned} \tag{71}$$

$$\begin{aligned} \tfrac{\partial v}{\partial t} + U(y)\tfrac{\partial v}{\partial x} &= -\tfrac{\partial p}{\partial y} + \tfrac{1}{Re_l}\left(\tfrac{\partial^2 v}{\partial x^2} + \tfrac{\partial^2 v}{\partial y^2}\right) \\ &\quad + \tfrac{1}{Re_t}\left(D(y)\tfrac{\partial^2 u}{\partial x \partial y} + \tfrac{\partial}{\partial y}(D(y)\tfrac{\partial v}{\partial y})\right). \end{aligned} \tag{72}$$

It is not entirely clear from the form of the equations what the correct number of boundary conditions is at an outflow boundary. However, following either the analysis of Halpern and Schatzmann [10] or Naughton [13] we seek two conditions. Often in numerical algorithms the somewhat awkward divergence equation is replaced by a Poisson equation for the pressure. Then, an additional boundary condition is needed. To guarantee that the velocity field is divergence free, this condition must in general ensure that the divergence is zero at the boundary. (For outflow boundaries Naughton has shown that this may be relaxed to a Neumann condition on the divergence.)

One possibility is to apply the boundary operator derived in the sections above to two of the perturbed variables. For example,

$$Bu = 0, \tag{73}$$

$$Bv = 0. \tag{74}$$

An alternate approach, which could also be applied to the stream function - vorticity formulation, is to introduce directly into the equations the scalings used to approximate the spatial Orr-Sommerfeld equation. In terms of the physical variables these are:

$$\frac{\partial}{\partial x} = O(\frac{1}{Re}), \tag{75}$$

$$\frac{\partial}{\partial t} = O(\frac{1}{Re}). \tag{76}$$

(Here Re is the turbulent or kinematic Reynolds number as appropriate.) The continuity equation, (70), may be integrated from a wall boundary to yield:

$$v = O(\frac{1}{Re}). \tag{77}$$

Differentiating (77) with respect to x yields:

$$\frac{\partial v}{\partial x} = O(\frac{1}{Re^2}), \tag{78}$$

while substituting it into (72) along with the scalings leads to:

$$\frac{\partial p}{\partial y} = O(\frac{1}{Re^2}). \tag{79}$$

Dropping the $O(\frac{1}{Re^2})$ terms results in equations which could be used as boundary conditions. Unfortunately, the pressure condition is difficult to analyze using energy methods. To rectify this we add to it another $O(\frac{1}{Re^2})$ term and integrate with respect to y:

$$p - (\frac{1}{Re_l} + \frac{1}{Re_t}D(y))\frac{\partial u}{\partial x} = \Phi(t) + O(\frac{1}{Re^2}). \tag{80}$$

This corresponds to the so called normal constraint of [10]. The function $\Phi(t)$ corresponds to the arbitrary constant which may be added to p. For simplicity we take $\Phi(t) = 0$. This leads to the following boundary conditions:

$$\frac{\partial v}{\partial x} = 0, \tag{81}$$

$$p - (\frac{1}{Re_l} + \frac{1}{Re_t}D(y))\frac{\partial u}{\partial x} = 0. \tag{82}$$

For solvers which use the Poisson equation for p this must be supplemented by either $\frac{\partial u}{\partial x} + \frac{\partial v}{\partial y} = 0$ or $\frac{\partial^2 v}{\partial x^2} = 0$.

Equations (81-82) are discussed in [13] where they are called Type 3 conditions. Energy estimates independent of Re are given there for the half channel laminar flow problem ($D = 0$) using these conditions and linearizations about an arbitrary velocity field with outflow. A simple generalization of Naughton's estimates holds in the case of turbulent flow.

It is interesting to compare (81-82) with the conditions given in [10]. The equation for v is common to both works. In [10] equation (82) is replaced by a more complicated relationship between p and the velocities which is nonlocal in space.

In the future we plan to carry out numerical experiments which test these conditions as well as to consider the problem of deriving error estimates. Among other interesting questions to be studied are the application of these ideas to viscous, compressible flows, their use in the simulation of interesting unsteady flows and their generalization to problems in three dimensions. We note that the reduction of domain size allowed by the use of asymptotic boundary conditions is of increasing importance for three dimensional simulations. In the three dimensional case the reduction in effort resulting from the use of the approximate eigenvalue problem or the direct use of the scalings would also be most keenly felt.

References

[1] S. Abarbanel, A. Bayliss and L. Lustman, "Non-reflecting boundary conditions for the compressible Navier-Stokes equations", ICASE Report No. 86-9, (1986).

[2] G. Ache, "Computational boundary conditions for the incompressible Navier-Stokes equations in channels and pipes", CMS TSR No. 88-12, Dept. of Computer Sciences, University of Wisconsin, Madison, WI, (1987).

[3] J. Bramley and S. Dennis, "The calculation of eigenvalues for the stationary perturbation of Poiseuille flow", *J. Comp. Phys.*, 47, (1982), 179-198.

[4] C. Canuto, M. Hussaini, A. Quarteroni and T. Zang, *Spectral Methods in Fluid Dynamics*, Springer-Verlag, (1988).

[5] G. Danabasoglu, S. Biringen and C.L. Street, "Numerical simulation of spatially evolving instability", appearing in *NASA Langley Transition Workshop Proceedings*, Springer-Verlag, (1989).

[6] P. Drazin and W. Reid, *Hydrodynamic Stability*, Cambridge University Press, (1981).

[7] H. Fasel, "Investigation of the stability of boundary layers by a finite-difference model of the Navier-Stokes equations", *J. Fluid Mech.*, 78, (1976), 355-383.

[8] T. Hagstrom, "Asymptotic boundary conditions for dissipative waves: General theory", *Math. Comp.*, submitted for publication.

[9] L. Halpern, "Artificial boundary conditions for the linear advection diffusion equation", *Math. Comp.*, 46, (1986), 425-438.

[10] L. Halpern and M. Schatzman, "Artificial boundary conditions for viscous incompressible flows", *SIAM J. Math. Anal.*, 20, (1989), 308-353.

[11] R. **Higdon,** "Numerical absorbing boundary conditions for the wave equation", *Math. Comp.*, **49,** (1987), 65-90.

[12] T. Kato, *Perturbation Theory for Linear Operators*, Springer-Verlag, (1980).

[13] M. Naughton, Doctoral Dissertation, Dept. of Applied Mathematics, California Institute of Technology, (1986).

[14] M. Stanisic, *The Mathematical Theory of Turbulence*, Springer-Verlag, (1988).

NASA
National Aeronautics and Space Administration

Report Documentation Page

1. Report No.	2. Government Accession No.	3. Recipient's Catalog No.
NASA TM-102510 ICOMP-90-05		

4. Title and Subtitle	5. Report Date
Conditions at the Downstream Boundary for Simulations of Viscous Incompressible Flow	February 1990
	6. Performing Organization Code

7. Author(s)	8. Performing Organization Report No.
Thomas Hagstrom	E-5312
	10. Work Unit No.
	505-62-21

9. Performing Organization Name and Address	11. Contract or Grant No.
National Aeronautics and Space Administration Lewis Research Center Cleveland, Ohio 44135-3191	
	13. Type of Report and Period Covered
	Technical Memorandum

12. Sponsoring Agency Name and Address	14. Sponsoring Agency Code
National Aeronautics and Space Administration Washington, D.C. 20546-0001	

15. Supplementary Notes

Thomas Hagstrom, Dept. of Applied Mathematics and Statistics, State University of New York at Stony Brook, Stony Brook, New York 11794 and Institute for Computational Mechanics in Propulsion (work funded by Space Act Agreement C-99066-G). Space Act Monitor, Louis A. Povinelli.

16. Abstract

The paper specification of boundary conditions at artificial boundaries for the simulation of time-dependent fluid flows has long been a matter of controversy. In this work we apply the general theory of asymptotic boundary conditions for dissipative waves, developed by the author in [8], to the design of simple, accurate conditions at a downstream boundary for incompressible flows. For Reynolds numbers far enough below the critical value for linear stability, a scaling is introduced which greatly simplifies the construction of the asymptotic conditions. Numerical experiments with the nonlinear dynamics of vortical disturbances to plane Poiseuille flow are presented which illustrate the accuracy of our approach. The consequences of directly applying the scalings to the equations are also considered.

17. Key Words (Suggested by Author(s))	18. Distribution Statement
Navier-Stokes equations Boundary conditions Asymptotic expansions Unsteady flow	Unclassified – Unlimited Subject Category 64

19. Security Classif. (of this report)	20. Security Classif. (of this page)	21. No. of pages	22. Price*
Unclassified	Unclassified	26	A03

*For sale by the National Technical Information Service, Springfield, Virginia 22161